

All-optical technique for stabilization of an external cavity laser diode: numerical and experimental demonstrations

F. Rogister^{*a}, D. W. Sukow^b, P. Mégret^a, O. Deparis^a, A. Gavrielides^c, M. Blondel^a

^aFaculte Polytechnique de Mons, Advanced Research in Optics group,
31 Boulevard Dolez, B-7000 Mons, Belgium

^bWashington and Lee University, Department of Physics and Engineering,
Lexington, Virginia 24450, USA

^cAir Force Research Laboratory AFRL/DELO, Nonlinear Optics Group,
3550 Aberdeen Avenue SE, Kirtland AFB, NM 87117-5776, USA

ABSTRACT

We demonstrate numerically and experimentally that low-frequency fluctuations (LFF) in a laser diode subject to delayed optical feedback can be suppressed or stabilized by a second optical feedback with a short delay. The second feedback suppresses LFF by shifting antimodes far away from the external cavity modes in phase space, or by making them disappear, with the consequence that the crises that induce the power dropouts are no longer possible. Moreover, as the second feedback strength increases, the laser undergoes a bifurcation cascade with successive regions where it exhibits chaos or LFF and regions where it locks to a newly-born stable maximum gain mode. This all-optical stabilization technique is easier to implement from an experimental point of view than many existing methods since it does not require modification of any laser parameters or of the first optical feedback.

Keywords: semiconductor laser, optical feedback, chaos stabilization

1. INTRODUCTION

External optical feedback is known to reduce considerably the linewidth of a laser diode [1] but it can also degrade its temporal and spectral characteristics by inducing a wide variety of dynamic instabilities such as chaos [2], coherence collapse [3] and low frequency fluctuations (LFF) [4].

The coherence collapse regime is observed in a laser diode pumped well above threshold and subject to a moderate amount of optical feedback. It is characterized by a huge broadening of the optical linewidth from typically 100 MHz to several tens of GHz. The LFF regime is also observed for moderate level of optical feedback but generally when the laser diode is pumped close to its solitary threshold. The dominant features of this regime are sudden power drop-outs followed by gradual, stepwise recoveries. While the LFF phenomenon was already observed in 1977 [4], its origins remained obscure for almost two decades. Several theories have been proposed to explain the physical mechanisms underlying LFF. The most generally accepted theory has been proposed by Sano [5] who showed through analytical and numerical investigation of the Lang-Kobayashi equations [6] that LFF power dropouts are due to crises between external cavity modes and antimodes, leading to collisions of the system trajectory in phase space with the saddle-type antimodes. Sano also demonstrated that each

* Correspondence: Email: Rogister@telecom.fpms.ac.be; Telephone: 32 65 37 41 98; Fax: 32 65 37 41 99

dropout is preceded by a chaotic itinerancy of the trajectory among attractor ruins of external cavity modes, with a drift towards the maximum gain mode.

Since optical-feedback-induced instabilities degrade the laser diode's performances, it is highly desirable to control such behaviors, and various methods have been proposed [7-9]. However, in most of these methods, the control is performed by adjusting one or several parameters of the laser (e.g. the injection current) or of the optical feedback (e.g. the feedback phase). However, these system parameters may not be modified easily in practice.

An alternative method that uses a second external optical feedback [9] was proposed to stabilize a chaotic laser diode pumped far above threshold in the coherence collapse regime. Rogister *et al.* [10] have investigated the same scheme but when the laser is pumped close to threshold, paying close attention to the steady-state solutions. Relying on Sano's theory of LFF, the method uses a second delayed optical feedback to suppress LFF by destroying the antimodes that are responsible for the crises, or by pushing them far away from the external cavity modes with the consequence that the drop-outs can no longer occur. Stabilization is achieved as the laser locks onto new, stable maximum gain modes that are created as the second feedback strength increases. Important advantages of this method are that stabilization may in theory be achieved regardless of the first feedback strength and that it does not require modification of any laser parameters or of the first optical feedback.

In this paper, we report the first experimental realization of this novel all-optical control method. In good agreement with previous theoretical results [10], we show that LFF is suppressed by destroying the antimodes that are responsible for the crises and that stabilization is achieved as the laser locks onto new stable maximum gain modes that are created as the second feedback strength increases.

The paper is organized as follows. In Section 2, we present the extension of the Lang-Kobayashi equations to the double-feedback problem and we review the main theoretical results presented in Ref. 10. In Section 3, we describe our experimental setup and we report on the experimental suppression of LFF and stabilization of the laser.

2. THEORETICAL ANALYSIS

2.1. Model and steady state solutions

The well-known Lang-Kobayashi equations [6] are generally considered to give a valid approximation of a single-mode laser subject to low and moderate optical feedback from an external cavity. This model may be extended to the problem of a laser diode subject to optical feedback from a double cavity (Fig. 1) by including a second delay term in the rate equation for the electric field. The equations for the slowly varying complex electric field $E(t) = A(t)\exp[i\phi(t)]$ and the normalized excess carrier number $N(t)$ formulated in dimensionless form [11] read:

$$E' = (1 + i\alpha)NE + \kappa_1 E(t - \tau_1) e^{-i\Omega\tau_1} + \kappa_2 E(t - \tau_2) e^{-i\Omega\tau_2}, \quad (1)$$

$$TN' = P - N - (1 + 2N)|E|^2. \quad (2)$$

where primes indicate derivatives with respect to time t measured in units of the photon lifetime τ_p , α is the linewidth enhancement factor, Ω is the normalized angular frequency of the solitary laser, P is the dimensionless pumping current above solitary laser threshold, and T is the ratio of carrier lifetime to photon lifetime. The parameters κ_1 and κ_2 are the normalized feedback strengths of the first and second external cavities, respectively, and τ_1 and τ_2 are the corresponding round-trip times normalized to τ_p .

Eqs. (1) and (2) have steady-state solutions that, written in the form $E(t) = A_s \exp[i(\Delta - \Omega)t]$ and $N(t) = N_s$, satisfy

$$\Delta = \Omega - \kappa_1 \left(\alpha \cos(\Delta\tau_1) + \sin(\Delta\tau_1) \right) - \kappa_2 \left(\alpha \cos(\Delta\tau_2) + \sin(\Delta\tau_2) \right) \quad (3)$$

$$A_s^2 = \frac{P - N_s}{1 + 2N_s} \quad (4)$$

$$N_s = -\kappa_1 \cos(\Delta\tau_1) - \kappa_2 \cos(\Delta\tau_2) \quad (5)$$

where Δ is a stationary angular frequency and the corresponding A_s and N_s are constants.

Steady-state solutions correspond to interferences between the electric field inside the solitary laser cavity and the electric field that is fed back into laser from the two external cavities. As in the single-feedback case, steady-state solutions associated with constructive interferences are called external cavity modes (ECM), whereas steady-state solutions associated with destructive interferences are called antimodes. The latter are always unstable and satisfy the condition $d\Omega/d\Delta < 0$ [12].

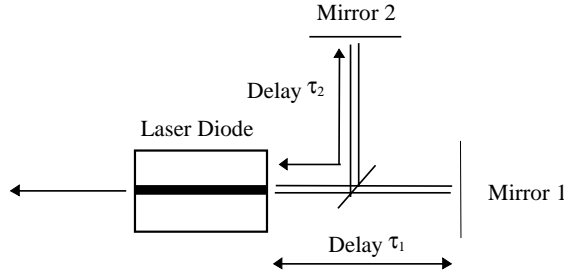


Fig. 1: Proposed configuration for suppressing LFF and for stabilizing the laser diode.

2.2. Numerical results

For numerical studies, we use typical parameters of a laser diode pumped close to threshold [8]: $\alpha = 4$, $T = 1000$, $P = 0.001$. In this section, the strength, the delay and the phase of the first optical feedback are such that LFF is observed numerically when there is no second optical feedback ($\kappa_2 = 0$): $\kappa_1 = 4.6 \times 10^{-3}$, $\tau_1 = 1000$ and $\Omega\tau_1 = -1.45$. The delay and the phase of the second optical feedback are $\tau_2 = 200$ and $\Omega\tau_2 = 0.8$ respectively. In all this section, the strength of the second feedback is the only variable parameter.

We use Eqs. (3) and (4) to calculate Fig. 2, which shows the evolution of the product of the stationary angular frequencies and the first feedback delay, $\Delta\tau_1$, with respect to κ_2 . As with the single optical feedback problem, antimodes and external cavity modes are created in pairs through saddle-node bifurcations as the second feedback strength is increased. But unlike the single feedback problem, pairs of steady-state solutions can also disappear in the double feedback configuration when κ_2 increases.

The coupled nonlinear rate equations (1) and (2) are numerically solved using a fourth-order Runge-Kutta algorithm. The bifurcation diagram of the phase difference function $\phi(\tau) - \phi(t - \tau_1) + \Omega\tau_1$ with κ_2 as the bifurcation parameter is presented in Fig. 3. The phase difference function reduces to $\Delta\tau_1$ for stationary behaviors and it can be directly compared with Fig. 2. In the absence of the second optical feedback (i.e. $\kappa_2 = 0$) and for very low values of its strength, the laser displays LFF dynamics. But as κ_2 increases, the antinode responsible for the LFF crises and the maximum gain mode come close together and finally disappear for $\kappa_2 = 4.5 \times 10^{-4}$. LFF is thereby suppressed since crises are no longer possible and the laser locks into the chaotic attractor of the nearest external cavity mode. The chaotic behavior is observed in a very small range of κ_2 , and as the strength of the second feedback increases, quasiperiodic (from $\kappa_2 = 0.5 \times 10^{-3}$ to 0.8×10^{-3}) and periodic behaviors (from $\kappa_2 = 0.8 \times 10^{-3}$ to 3×10^{-3}) are successively observed. Finally the laser stabilizes and locks onto a new external cavity mode from $\kappa_2 = 3.1 \times 10^{-3}$ to 5.6×10^{-3} . For further increases of κ_2 , the laser undergoes a cascade of bifurcations with successive regions of unstable behaviors such as periodic and quasiperiodic behaviors, chaos, and LFF where the laser operates in multiple external cavity modes (e.g. from $\kappa_2 = 6.4 \times 10^{-3}$ to 8.3×10^{-3} and from $\kappa_2 = 14.3 \times 10^{-3}$ to 17.3×10^{-3}), alternating with regions of stable behaviors where the laser locks into new stable maximum gain modes (e.g. from $\kappa_2 = 8.3 \times 10^{-3}$ to 10.9×10^{-3}).

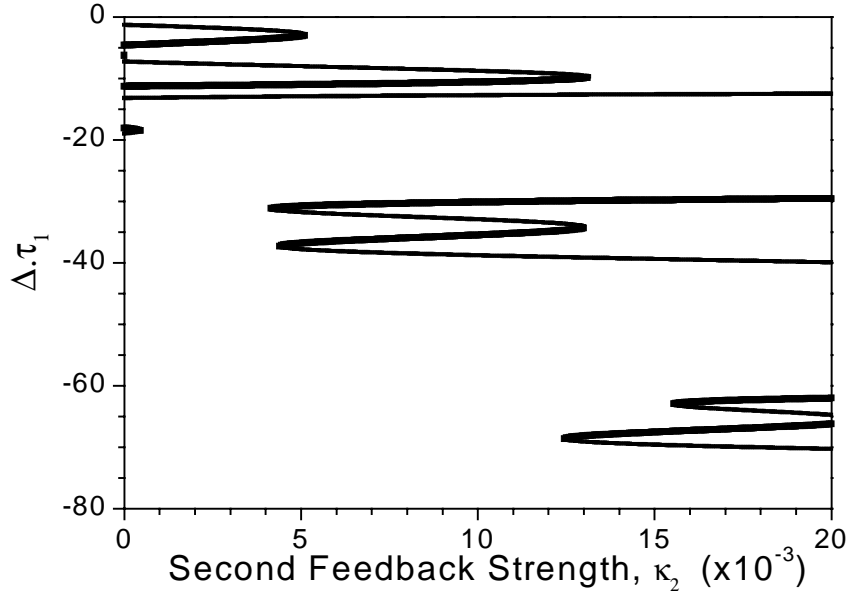


Fig. 2: Stationary angular frequencies Δ as a function of κ_2 . Thick lines correspond to antimodes, thin lines correspond to external cavity modes. Pairs of external cavity modes and antimodes disappear for $\kappa_2 = 4.5 \times 10^{-4}$ and $\kappa_2 = 13 \times 10^{-3}$.

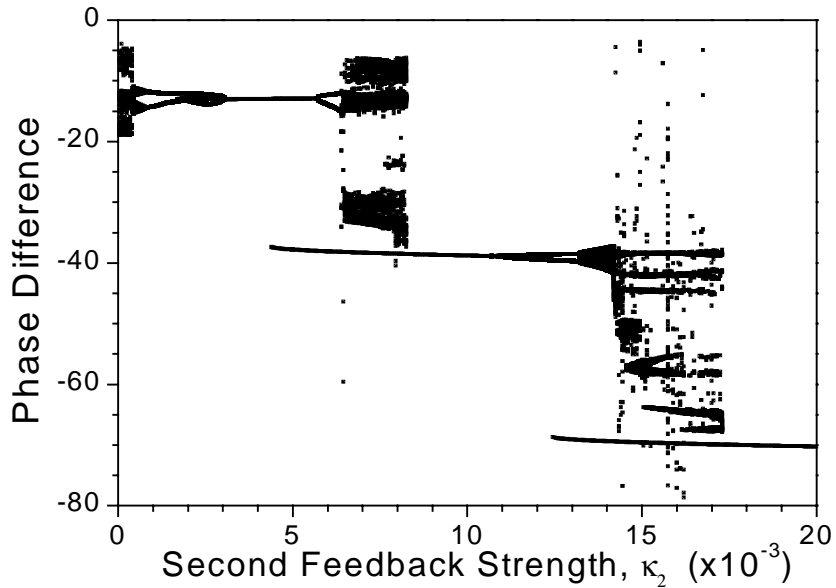


Fig. 3: Bifurcation diagram of the phase difference function $\phi(\tau) - \phi(t - \tau_l) + \Omega\tau_l$ with the strength of the second optical feedback as the bifurcation parameter. LFF is suppressed for $\kappa_2 = 4.5 \times 10^{-4}$. The laser is stabilized from $\kappa_2 = 3.1 \times 10^{-3}$ to $\kappa_2 = 5.6 \times 10^{-3}$ and from $\kappa_2 = 8.3 \times 10^{-3}$ to $\kappa_2 = 10.9 \times 10^{-3}$.

The stabilizing effect of the second optical feedback on the laser dynamics can also be illustrated by showing the corresponding optical spectra (Fig. 4) for different steps in the bifurcation cascade. The optical spectra are calculated from time series of the electric field, convolved with the spectral response of the Fabry-Perot interferometer used in the experiment.

Chaotic itinerancies of the system trajectory among external cavity modes are characterized by several broad sidebands located at the external cavity modes spacing in the optical spectra [Fig. 4 traces (a), (c) and (e)]. By contrast, stable behaviors are revealed in the optical spectra by single narrow lines [Fig. 4 traces (b), (d), and (f)] as the laser locks into stable external cavity modes. In contrast to the first stabilization of the laser that occurs after the LFF suppression [Fig. 4 trace (b)], the next laser stabilizations in newly-created maximum gain modes are characterized in the optical spectrum by large shifts to the lower frequencies [Fig. 4 traces (d), and (f)].

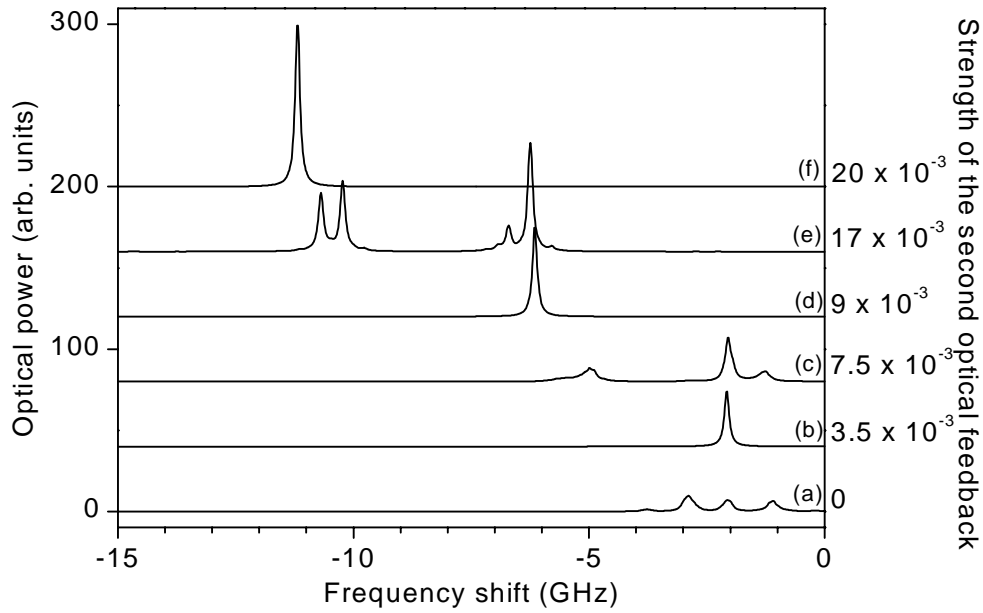


Fig. 4: Calculated optical spectra for different values of κ_2 . LFF regimes are revealed by the presence of multiple broad sidebands in the optical spectra. Stable behaviors are characterized by single narrow peaks. In this figure, optical spectra are calculated from time series of the electric field and smoothed by the spectral response of the Fabry-Perot interferometer used in the experiment.

2.3. Influence of the linewidth enhancement factor

It is well known that the linewidth enhancement factor is of great importance for the dynamical characteristics of the laser diode. In the LFF regime, the linewidth enhancement factor is responsible for the drift of the system trajectory towards the maximum gain mode where the crises with antimodes occur [13]. Similarly to the single optical feedback problem [14], the overall number of external cavity modes and antimodes increases as α increases while the distance between them in phase space, in particular near the maximum gain mode, decreases. As a consequence the collision of attractor ruins of external cavity modes with antimodes and therefore LFF crises are more probable when α is large. We have thus investigated the sensitivity of our stabilization technique to different values of α . For $\alpha = 4$, we have observed that stabilization occurs regardless of the strength of the first feedback and in a broad range of the second feedback delay. However for greater values of α ($\alpha = 5-6$), delay and phase of the second feedback must be carefully chosen to observe stabilization.

3. EXPERIMENT

3.1. Experimental setup

The experimental setup is illustrated in Fig. 5. We use a SDL-5301 laser diode operating at the wavelength $\lambda=780$ nm. The temperature-stabilized laser is biased at a pump current $I = 25.0$ mA, just below solitary threshold $I_{th} = 25.2$ mA. The laser beam is collimated by an antireflection coated lens (CL) and directed to a holographic grating (GR). The zeroth order diffracted by the grating is used to monitor the system's behavior. The first order of diffraction goes into the double cavity, which is formed by a non-polarizing beamsplitter (NPBS) and two 99% reflectivity mirrors. The double cavity is shielded from parasitic feedback from the detection branch by an optical isolator (ISO). External cavity optical lengths are $L_1 = 21$ cm and $L_2 = 19$ cm, respectively. The grating has 1200 lines per mm and is oriented at 45° with respect to the incident beam. Provided that the two mirrors are properly tilted, the grating narrows the cavity bandwidth to 50 GHz and restricts the laser diode to oscillate in only one of its longitudinal mode. The laser output is monitored using a scanning Fabry-Perot interferometer (Newport SR-240C, free spectral range of 2000 GHz, finesse > 17000) and a fast ac-coupled photodiode (Hamamatsu C4258, 8 GHz bandwidth). The photodiode signal is amplified and connected to a RF spectrum analyzer (HP 8596E) and a 500 MHz bandwidth digitizer (Tektronix RTD 720). The limited bandwidth of the digitizer allows the detection of the slow envelope of the optical power dynamics and the power drop-outs that characterize the LFF regime. The feedback strengths of each external cavity are controlled independently by means of a polarizing beamsplitter (PBS) and two polarizers (POL). They are characterized through the fractional threshold reduction $\Delta I = (I_{th} - I) / I_{th}$ induced by each cavity acting alone.

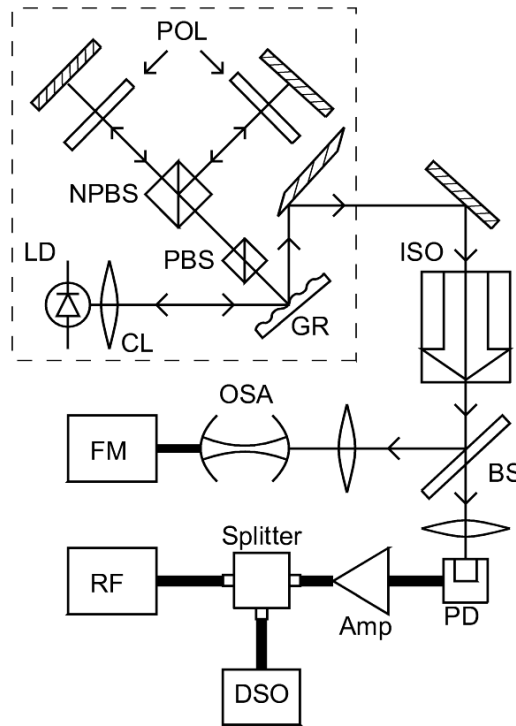


Fig. 5: Experimental setup

3.2. Experimental suppression of the LFF regime and stabilization of the laser

Figure 6 shows the experimentally observed optical spectra as a function of ΔI_2 , the threshold reduction due to the second cavity only. The horizontal axis has its origin at the frequency of the first mode that lases as the strength of the first feedback increases from zero when there is no second feedback. In the figure, the strength of the first feedback is fixed corresponding to a threshold reduction $\Delta I_1 = 7.1\%$ such that the laser displays LFF in seven external cavity modes when the laser is not subjected to a second feedback [trace(a)]. Increasing slightly the strength of the second feedback [$\Delta I_2 = 0.44\%$, trace (b)] results in the stabilization of the sixth external cavity mode of the *first* cavity. By comparison with

the calculated optical spectra (Fig. 4), we attribute this first stabilization to the destruction of the antimode responsible for the LFF crises since, in this case, we do not observe a large frequency shift to lower frequencies. For $\Delta I_2=1.58\%$ [trace (c)], the system loses stability, and once again displays LFF. For a threshold reduction of $\Delta I_2=6.42\%$ [trace (d)] the optical spectrum exhibits two peaks whose origin is discussed in the Section 3.3, below. Increasing further the second feedback strength [trace (e)], the system exhibits complex dynamics until $\Delta I_2=10.4\%$ [trace (f)] where the laser again becomes stable. We interpret this as a locking of the system onto a newly-created, stable maximum gain mode which is well-separated in frequency from the original seven external cavity modes of the first cavity. Further increases of the second feedback strength lead to a continuation of this pattern, with stabilization of increasingly distant modes interspersed with regions of complex behavior in agreement with numerical results presented in the previous section (Figs. 2-4).

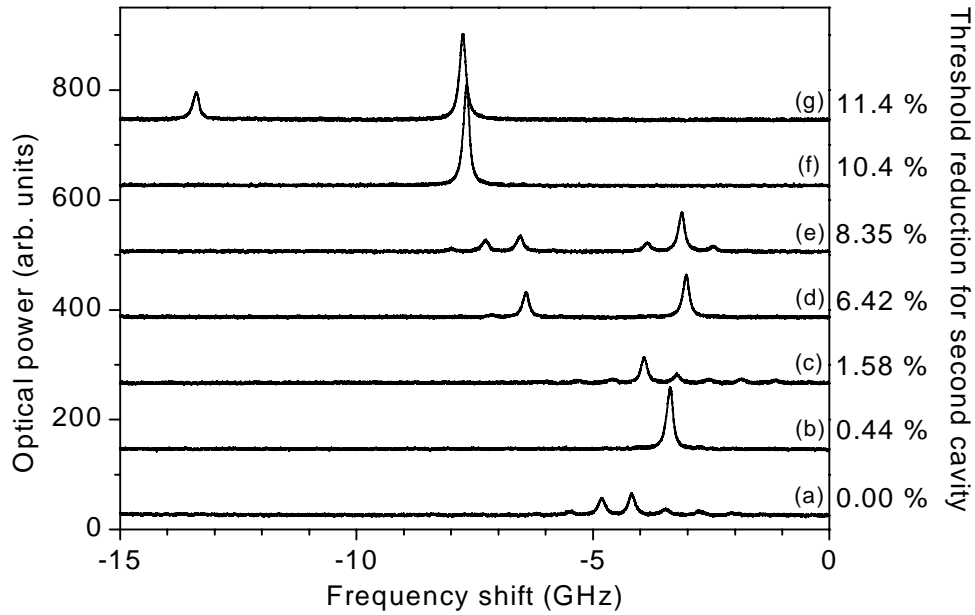


Fig. 6: Experimental optical spectra measured in the double-cavity configuration as a function of the threshold reduction ΔI_2 due to the second feedback strength. LFF is observed in the absence of the second feedback [trace (a)]. Increase of the second feedback strength leads to stabilization [traces (b) and (f)] interspersed with unstable regions [traces (c)-(e) and (g)].

Figs. 7 and 8 present time series and RF spectra corresponding to the two first steps in the bifurcation cascade. When the laser is subject to the first optical feedback only, the power clearly exhibits strong drop-outs [Fig. 7 (a)] and the RF spectrum presents peaks at multiples of the first external cavity frequency [Fig. 7 (b)]. When the laser is stabilized by means of the second feedback, the intensity shows only small fluctuations that are caused by the spontaneous emission noise [Fig. 8 (a)] and the corresponding RF spectrum is flat [Fig. 8 (b)]. We have observed that the control is robust, limited only by the mechanical stability of the system. Furthermore, it works for every first feedback strength accessible in our experiment.

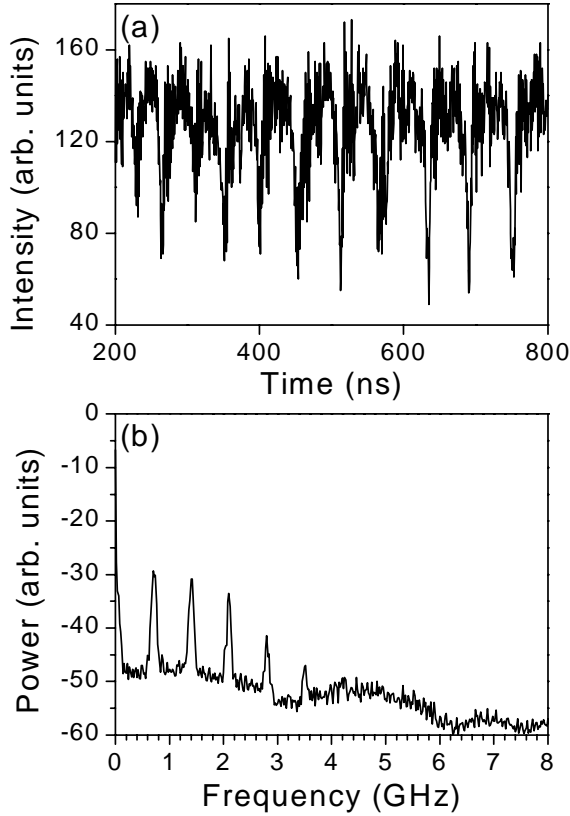


Fig. 7: LFF is observed in the absence of second optical feedback ($\Delta I_2 = 0\%$). (a) Intensity time trace. (b) RF spectrum

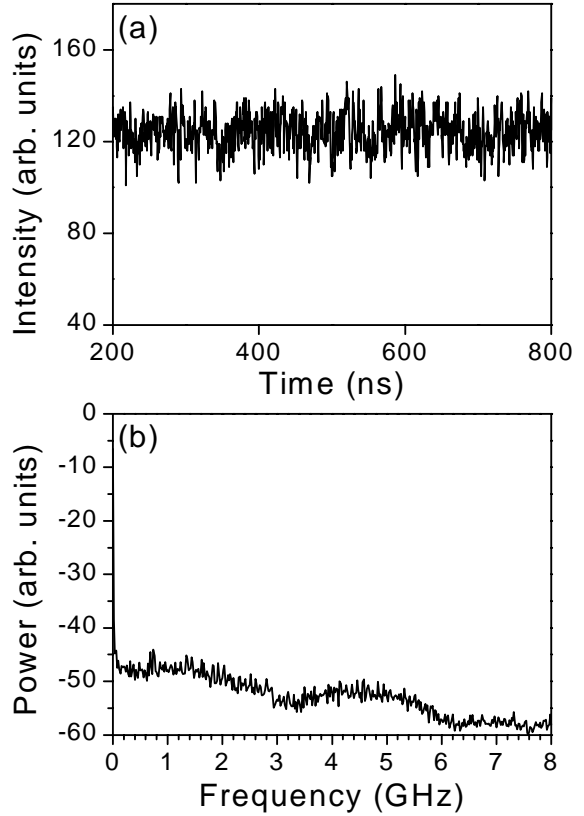


Fig. 8: Stabilization of the laser by means of the second optical feedback ($\Delta I_2 = 0.44\%$). (a) Intensity time trace. (b) RF spectrum.

Figure 9 illustrates that it is the joint action of the two optical feedbacks that produces stabilization of the laser. In Fig. 9, optical and RF spectra are recorded when the laser is subject to feedback from the first cavity alone [traces (a) and (b)], from the second cavity alone [traces (c) and (d)], and from both cavities acting in concert [traces (e) and (f)]. While the laser suffers from LFF when it is subject to feedback from the first or the second cavity alone (as revealed by the presence of broad sidebands in the optical spectra and peaks at multiples of external cavities frequencies), it stabilizes when it is subject to feedback from both cavities acting together; in this case, the optical spectrum exhibits a single narrow peak and the RF spectrum is flat.

3.3. High-frequency oscillations

The RF spectra exhibit a single sharp peak at 5 GHz when two sharp peaks are present simultaneously in the optical spectra [Fig. 6 (d) and (g)]. We attribute these observations to high-frequency periodic behaviors. Periodic behaviors with similar frequencies can be numerically found with Eqs. (1) and (2) for adequate parameters values. Such high frequencies are unusual in laser diodes pumped close to threshold and subjected to a single optical feedback; oscillations at the external cavity frequency [15] are typically expected. Our observations may be interpreted as the result of a beating between two external cavity modes, a phenomenon studied numerically by Tager and Petermann [16] in the case of laser diode subject to a single optical feedback.

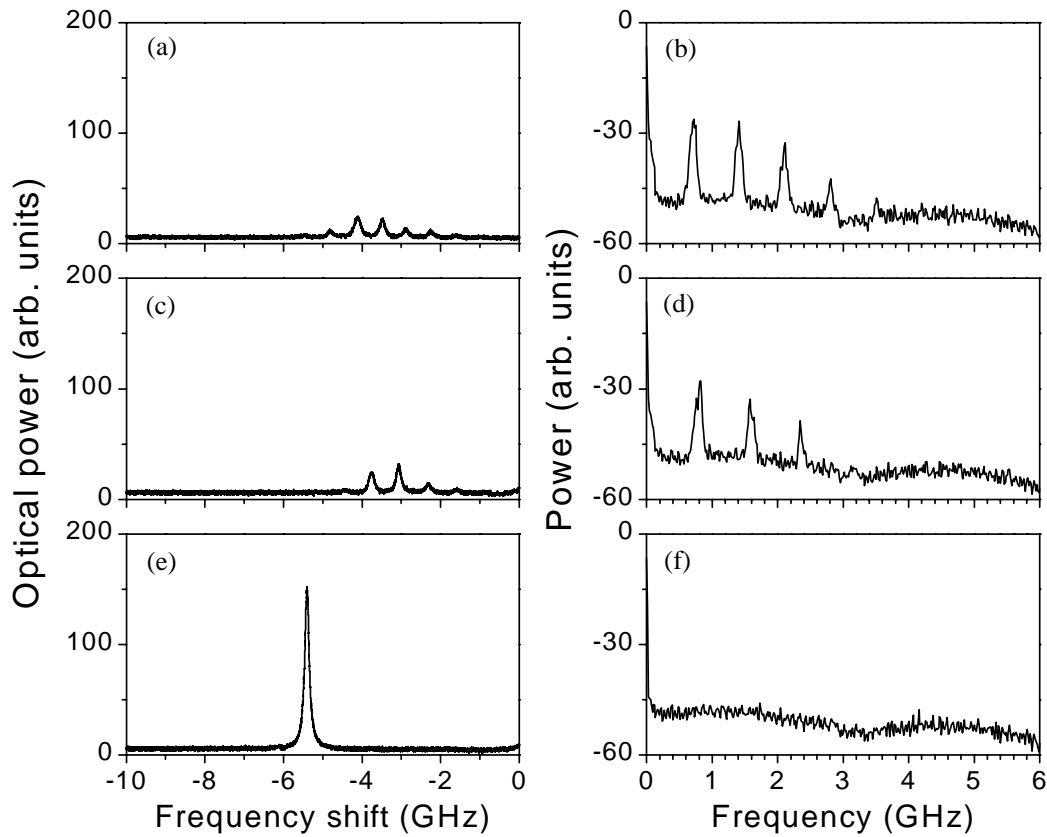


Fig. 9: Experimental optical and RF spectra recorded when the laser is subject to feedback from the first cavity alone [traces (a) and (b)], from the second cavity alone [traces (c) and (d)] and from both cavities [traces (e) and (f)].

4. CONCLUSION

We have demonstrated numerically and experimentally an all-optical stabilization technique for an external cavity laser diode. This method uses a second delayed optical feedback that suppresses LFF by destroying antimodes responsible for the crises or by pushing them far away from external cavity modes, and stabilizes the laser through creation of new maximum gain modes. Unlike many existing methods of control or of stabilization, our technique does not require modification of the laser or first optical feedback parameters. According to numerical simulations, stabilization may be achieved regardless of the strength of the first feedback and in a broad range of the second feedback delay for low values of the linewidth enhancement factor (i.e. $\alpha \sim 4$). Stabilization is still possible for larger values of α ($\alpha \sim 5 - 6$), but for appropriate second feedback delay and phase. In our experiment, we observed that our stabilization technique works for every accessible first feedback strength.

ACKNOWLEDGMENTS

This work is funded by the Inter-University Attraction Pole program (IAP IV/07) of the Belgian government. DWS acknowledges the support of the National Research Council and US Air Force Office of Scientific Research.

REFERENCES

1. G. P. Agrawal and N. K. Dutta, *Long-Wavelength Semiconductor Lasers*. New York: Van Nostrand Reinhold, 1986.
2. J. Mørk, B. Tromborg, and J. Mark, "Chaos in semiconductor lasers with optical feedback: theory and experiment," *IEEE J. Quantum Electron.*, vol. 28, pp. 93-108, 1992.
3. D. Lenstra, B. H. Verbeek, and A. J. den Boef, "Coherence collapse in single-mode semiconductor lasers due to optical feedback," *IEEE J. Quantum Electron.*, vol. QE-21, pp. 674-679, 1985.
4. C. Risch and C. Voumard, "Self-pulsation in the output intensity and spectrum of GaAs-AlGaAs cw diode lasers coupled to a frequency-selective external optical cavity," *J. Appl. Phys.*, vol. 48, pp. 2083-2085, 1977.
5. T. Sano, "Antimode dynamics and chaotic itinerancy in the coherence collapse of semiconductor lasers with optical feedback," *Phys. Rev. A*, vol. 50, pp. 2719-2726, 1994.
6. R. Lang and K. Kobayashi, "External optical feedback effects on semiconductor injection laser properties," *IEEE J. Quantum Electron.*, vol. QE-16, pp. 347-355, 1980.
7. J. Wieland, C. R. Mirasso, and D. Lenstra, "Prevention of coherence collapse in diode lasers by dynamic targeting," *Opt. Lett.*, vol. 22, pp. 469-471, 1997.
8. A. Hohl and A. Gavrielides, "Experimental control of a chaotic semiconductor laser," *Opt. Lett.*, vol. 23, pp. 1606-1608, 1998.
9. Y. Liu and J. Ohtsubo, "Dynamics and chaos stabilization of semiconductor lasers with optical feedback from an interferometer," *IEEE J. Quantum Electron.*, vol. 33, pp. 1163-1169, 1997.
10. F. Rogister, P. Mégret, O. Deparis, M. Blondel, and T. Erneux, "Suppression of low-frequency fluctuations and stabilization of a semiconductor laser subjected to optical feedback from a double cavity: theoretical results," *Opt. Lett.*, vol. 24, pp. 1218-1220, 1999.
11. P. M. Alsing, V. Kovanis, A. Gavrielides, and T. Erneux, "Lang and Kobayashi phase equation," *Phys. Rev. A*, vol. 53, pp. 4429-4434, 1996.
12. H. Olesen, J. H. Osmundsen, and B. Tromborg, "Nonlinear dynamics and spectral behavior for an external cavity laser," *IEEE J. Quantum Electron.*, vol. QE-22, pp. 762-773, 1986.
13. G. H. M. van Tartwijk, A. M. Levine, and D. Lenstra, "Sisyphus effect in semiconductor lasers with optical feedback," *IEEE J. Sel. Top. Quantum Electron.*, vol. 1, pp. 466-472, 1995.
14. T. Heil, I. Fischer, and W. Elsässer, "Influence of amplitude-phase coupling on the dynamics of semiconductor lasers subject to optical feedback," *Phys. Rev. A*, vol. 60, pp. 634-641, 1999.
15. G. Lythe, T. Erneux, A. Gavrielides, and V. Kovanis, "Low pump limit of the bifurcation to periodic intensities in a semiconductor laser subject to external optical feedback," *Phys. Rev. A*, vol. 55, pp. 4443-4448, 1999.
16. A. A. Tager and K. Petermann, "High-frequency oscillations and self-mode locking in short external-cavity laser diodes," *IEEE J. Quantum Electron.*, vol. 30, pp. 1553-1561, 1994.